Hindawi Publishing Corporation
Journal of Nanomaterials
Volume 2013, Article ID 361249, 7 pages
http://dx.doi.org/10.1155/2013/361249

Research Article

Effects of Surface Morphology of $ZnAl_2O_4$ Ceramic Materials on Osteoblastic Cells Responses

José Luis Suárez-Franco,[1] Manuel García-Hipólito,[2] Miguel Ángel Surárez-Rosales,[2] José Arturo Fernández-Pedrero,[1] Octavio Álvarez-Fregoso,[2] Julio Alberto Juárez-Islas,[2] and Marco Antonio Álvarez-Pérez[1,3]

[1] *Laboratorio de Bioingeniería de Tejidos, Facultad de Odontología, Universidad Nacional Autónoma de México, Coyoacán, 04510 Ciudad de México, DF, Mexico*
[2] *Instituto de Investigaciones en Materiales, Universidad Nacional Autónoma de México, Coyoacán, 04510 Ciudad de México, DF, Mexico*
[3] *Tissue Bioengineering Laboratory, Division of Research and Postgraduate Studies, Faculty of Dentistry, National Autonomous University of Mexico (UNAM), Circuito Exterior s/n, Coyoacan, 04510 Mexico City, DF, Mexico*

Correspondence should be addressed to Marco Antonio Álvarez-Pérez; marcoalv@unam.mx

Received 5 September 2012; Revised 16 January 2013; Accepted 17 January 2013

Academic Editor: Nabeen Kumar Shrestha

Ceramic scaffolds are widely studied in the tissue engineering field due to their potential in medical applications as bone substitutes or as bone-filling materials. The purpose of this study was to investigate the effect of surface morphology of nanostructure thin films of $ZnAl_2O_4$ prepared by spray pyrolysis and bulk pellets of polycrystalline $ZnAl_2O_4$ prepared by chemical coprecipitation reaction on the *in vitro* cell adhesion, viability, and cell-material interactions of osteoblastic cells. Our result showed that cell attachment was significantly enhanced from 60 to 80% on the $ZnAl_2O_4$ nanostructured material surface when compared with bulk ceramic surfaces. Moreover, our results showed that the balance of morphological properties of the thin film nanostructure ceramic improves cell-material interaction with enhanced spreading and filopodia with multiple cellular extensions on the surface of the ceramic and enhancing cell viability/proliferation in comparison with bulk ceramic surfaces used as control. Altogether, these results suggest that zinc aluminate nanostructured materials have a great potential to be used in dental implant and bone substitute applications.

1. Introduction

Oxide spinel material is a very large group of structurally related compounds [1], many of which are of considerable technological or geological importance [2]. Spinels exhibit a wide range of electronic and magnetic properties. The normal spinel is a typical example of a material with the general formula $(X)[Y]_2O_4$, where X and Y are divalent and trivalent ions, respectively, and the symbols () and [] refer to the 8 tetrahedral coordinated A sites and 16 octahedral coordinated B sites, respectively, within the cubic cell. $ZnAl_2O_4$ is an oxide spinel with a close-packed face centered cubic structure and Fd3 m space group symmetry [3]. Moreover, its band gap of 3.8 eV makes it transparent for light possessing wavelengths >320 nm; these characteristics allow to use it as a host lattice for applications in thin film electroluminescent displays, mechanooptical stress sensors, and stress imaging devices. On the other hand, this material has good catalytic properties such as cracking, dehydration, and dehydrogenation [4]. The spinel zinc aluminates have been widely used as ceramic and as catalytic material in chemical and petrochemical industries [5] and more recently as transparent conductor. Regarding the biological application potentials of this $ZnAl_2O_4$ ceramic material in thin films and in bulk are very scarce. The search for bone substitute is still a challenge to researchers. The composition, as well as the topography, of such materials is of importance for determining the biological response to such materials [6]. The roughness of materials

is considered to be important to predict interfacial behavior at the material-tissue interface and its interaction with the biological environment. Surface roughness influences cell bioactivity, being important in several bone formation stages, including adhesion, proliferation, differentiation, synthesis of bone matrix, maturation, and calcification of the tissue on the materials surface [7–10]. Besides, bioactivity or bioinertness could result in materials with different physical characteristic that could influence biological behavior [11, 12]. Recently, a number of studies have been carried out to investigate the Zn-doped ceramics as biomaterials in bone tissue engineering [13, 14]. Similar to calcium, zinc has long been recognized as an essential trace element for the proper maintenance of bone growth, with over 85% of the total body zinc residing in bone [15, 16]. Zn has a stimulatory effect on bone formation, and its deficiency has been associated with retardation and failure of bone growth in animals [17, 18]. Zn-substituted ceramics were found that modulate the attachment, proliferation, and differentiation of osteoblasts and modulate the activity of bone formation by the cells [19–21]. In this context, the aim of this study was to investigate the effect of surface morphology of nanostructured thin films of $ZnAl_2O_4$ prepared by spray pyrolysis and bulk pellets of polycrystalline $ZnAl_2O_4$ prepared by chemical coprecipitation reaction on the biological response of osteoblastic cells in order to evaluate the surface cell adhesion, spreading, cell viability process at *in vitro* cell culture and compare these results with respect to the different surface morphologies between a nanostructured thin film and a traditional polycrystalline ceramic surface.

2. Experimental Details

2.1. Synthesis and Characterization of $ZnAl_2O_4$ Material. The ultrasonic spray pyrolysis technique is a well-established process for depositing films. Some advantages of this process are as follow: a high deposition rate, the possibility to coat large areas, its low cost, its ease of operation, and the quality of the coatings obtained. Films of zinc aluminate were deposited by an ultrasonic spray pyrolysis technique described earlier [22]. Basically, this technique consists of an ultrasonic generator used to produce a mist from the spraying solution. This mist is carried to a hot substrate placed on a tin bath through a tubing setup using humid air as a carrier gas (10 liters/minute). When the mist of the solution gets in touch with the hot substrate, the solvents in the solution are vaporized producing a solid coating on the substrate. The nozzle in this system is localized approximately 1 cm above the substrate. The spraying solution consisted of 0.05 M zinc acetate and aluminum chloride in deionized water as solvent. The solution flow rate was 3 mL/minute for all cases. The substrate temperature (T_s) during deposition was in the range from 300°C to 550°C; the substrates used were Corning 7059 glass slides. The deposition time was adjusted (4 to 6 minutes) to deposit films with approximately the same thickness. The thickness of the films studied was about 5 μm as measured by a Sloan Dektak IIA profilometer. The chemical composition of the films was measured with a Leica-Cambridge electron microscope Mo. Stereoscan 440, equipped with a Beryllium window X-ray detector, using Energy Dispersive Spectroscopy (EDS). The standard used for the EDS measurements was the Multi-element X-ray Reference Standard (Microspec), Serial 0034, part no. 8160-53. The surface morphology was analyzed by means of the scanning electron microscopy (SEM) cited above. The crystalline structure features of the deposited films were analyzed by X-ray diffraction (XRD), using a Siemens D-5000 diffractometer with a wavelength radiation of 1.5406 Å (Cuk_α).

A very simple chemical precipitation process was used for the synthesis of zinc aluminate spinel powder. The start materials were $Zn(NO_3)_2 \cdot 6H_2O$ Sigma-Aldrich (98%) and $Al(NO_3)_3 \cdot 9H_2O$ Riedel-de Haën at 0.05 M blended in methanol. This simple process consists of three steps: (1) precursor material dissolution in a compatible solvent to form the precursor mixture, (2) solvent evaporation and solute precipitation, and (3) powder annealing. The initial mixture was heat treated at 250°C for 30 minutes to evaporate the solvent. The chemical agglomerates were grounded in an agate mortar to obtain fine powder, which was compressed to form a small disk with a dimension of 1.2 cm in diameter and a thickness of 0.13 cm. The applied pressure for pellets preparation was 150 Kg/cm^2. These pellets were annealed at T_a = 600°C, during 14 hours in air atmosphere.

The crystalline structure of these pellets was analyzed by X-ray diffraction (XRD) using a Bruker-D8 plus Diffractometer with CuK_α radiation at 1.5405 Å. Their chemical composition was measured using Energy Dispersive Spectroscopy (EDS) with a Cambridge-Leica electron microscope mod. Stereoscan 440 was equipped with a Beryllium window X-ray detector, and their surface topography was obtained by means of the above-mentioned SEM microscope.

2.2. Biological Response

2.2.1. Cell Culture. Biological assays were performed using human osteoblastic cells as reported previously [23]. For cell culture, human osteoblastic cells were cultured in 75 cm^2 cell culture flasks containing a Dulbecco's Modified Eagle Media (DMEM), supplemented with 10% fetal bovine serum (FBS) and antibiotic solution (streptomycin 100 μg/mL and penicillin 100 U/mL, Sigma Chem. Co). The cell cultures were incubated in a 100% humidified environment at 37°C in atmosphere of 95% air and 5% CO_2. Human osteoblastic cells on passage 4–6 were used for all the experimental procedures. In order to perform the *in vitro* cell response assays, all $ZnAl_2O_4$ bulk and 550°C nanostructured material surfaces were cleaned with distilled water and sterilized by exposure to UV light (λ = 254 nm, 300 uW/cm^2).

2.2.2. Cell Attachment. The cell adhesion of human osteoblastic cells onto $ZnAl_2O_4$ bulk and thin film nanostructure materials was evaluated using the vibrant cell adhesion assay kit (Molecular Probes). Human osteoblastic cells, cultured in a 75 cm^2 cell culture flask, were washed with phosphate-buffered saline (PBS) and incubated with calcein AM stock solution to a final concentration of 5×10^{-6} M in serum-free medium for 30 min. After incubation, the cells were washed

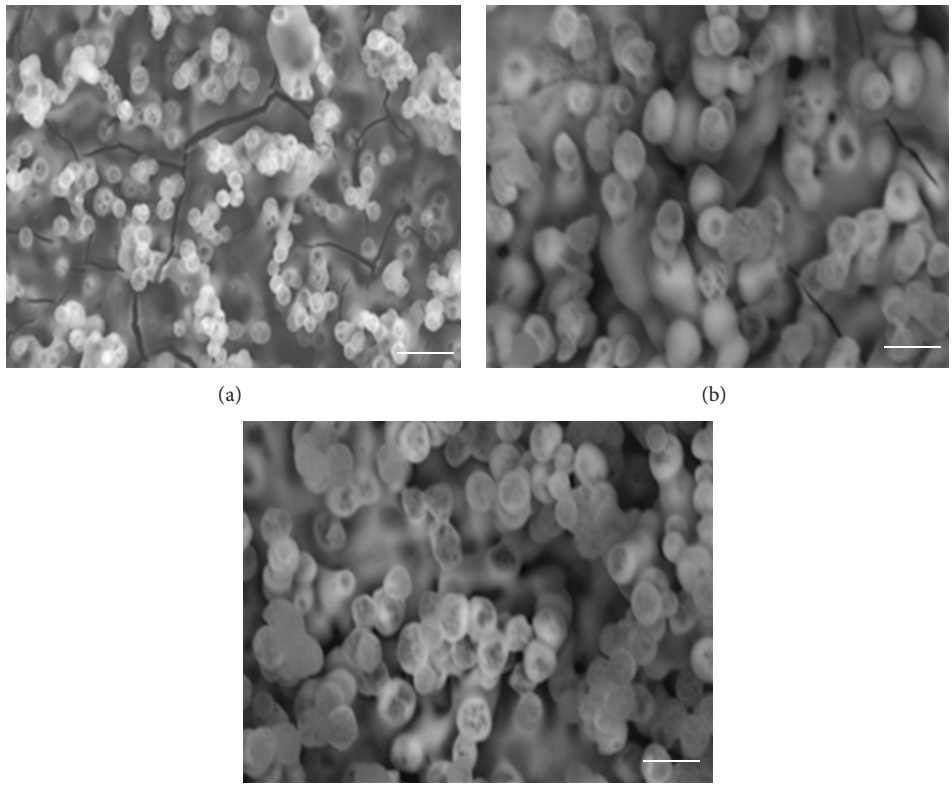

Figure 1: SEM micrographs of surface morphology of $ZnAl_2O_4$ films as a function of the T_s: (a) 300°C, (b) 450°C, and (c) 550°C. Bar = 100 nm.

with PBS, trypsinized, and the cell pellet was collected and diluted with DMEM culture medium to obtain the requisite cell concentration. The human osteoblastic cells at concentration of 1.5×10^3 cells/cm^2 were seeded onto $ZnAl_2O_4$ bulk and thin film nanostructured materials and incubated for 4 h and 24 h. The fluorescence was quantified using a fluorescein filter set with a Wallac Victor3 1420 spectrophotometer (Perkin-Elmer, Boston, MA, USA). The percentage cell adhesion was obtained by dividing the corrected (background subtracted) fluorescence of adherent cells by the total corrected fluorescence of control cells and multiplying by 100%. Conventional polystyrene 24-well culture plates were used as a control.

2.2.3. MTT Assay. Cell viability of human osteoblastic cells seeded at concentration of 1×10^4 cells/cm^2 onto $ZnAl_2O_4$ bulk and thin film nanostructured materials was checked by the MTT assay for 3, 5, and 7 days of culture. This assay is based on the ability of mitochondrial dehydrogenases of living cells to oxide a tetrazolium salt (3-[4, 5-dimethylthiazolyl-2-y]-2, 5-diphenyltetrazolium bromide), to an insoluble blue formazan product. The concentration of the blue formazan product is directly proportional to the number of metabolically active cells. The human osteoblastic cells seeded onto $ZnAl_2O_4$ bulk and thin film nanostructure materials at prescribed time were washed with PBS and incubated with fresh cultured medium containing 0.5 mg/mL of MTT for 4 h at 37°C in the dark. Then, the supernatant was removed and dimethyl sulfoxide (DMSO) was added to each well. After 60 minutes of slow shaking, the absorbance was quantified by spectrophotometry at 570 nm with a plate reader. The culture medium during experimental time was changed every other day with fresh media.

2.2.4. Cell Morphology. For cytoskeletal organization of the human osteoblastic cells cultured onto $ZnAl_2O_4$ bulk and thin film nanostructured materials, the cells were seeded at concentration of 1×10^3 cells/cm^2 and incubated for 24 hours in DMEM cultured medium. After 24 hours, the samples were washed with PBS and fixed with 4% paraformaldehyde for 10 minutes at room temperature (RT), permeabilized with 0.2% Triton X-100 for 5 minutes, washed twice with PBS and incubated with α-actin antibody diluted 1 : 100 in 0.2% of bovine serum albumin (BSA)-PBS for 1 h at RT. The cells were then gentile washed twice with 0.2% BSA-PBS and twice with PBS. Then, cells were incubated with FITC secondary antibody diluted 1 : 1000 in PBS for 1 hour. The cells were gentile washed with PBS and visualized by means of indirect immunofluorescence (Axiophot, Carl ZeissR, Germany).

2.2.5. Statistical Analysis. Data are presented as mean standard deviation. Statistical analysis was performed on adhesion and MTT assay results using Student's t-test, and P value <0.05 was considered significant.

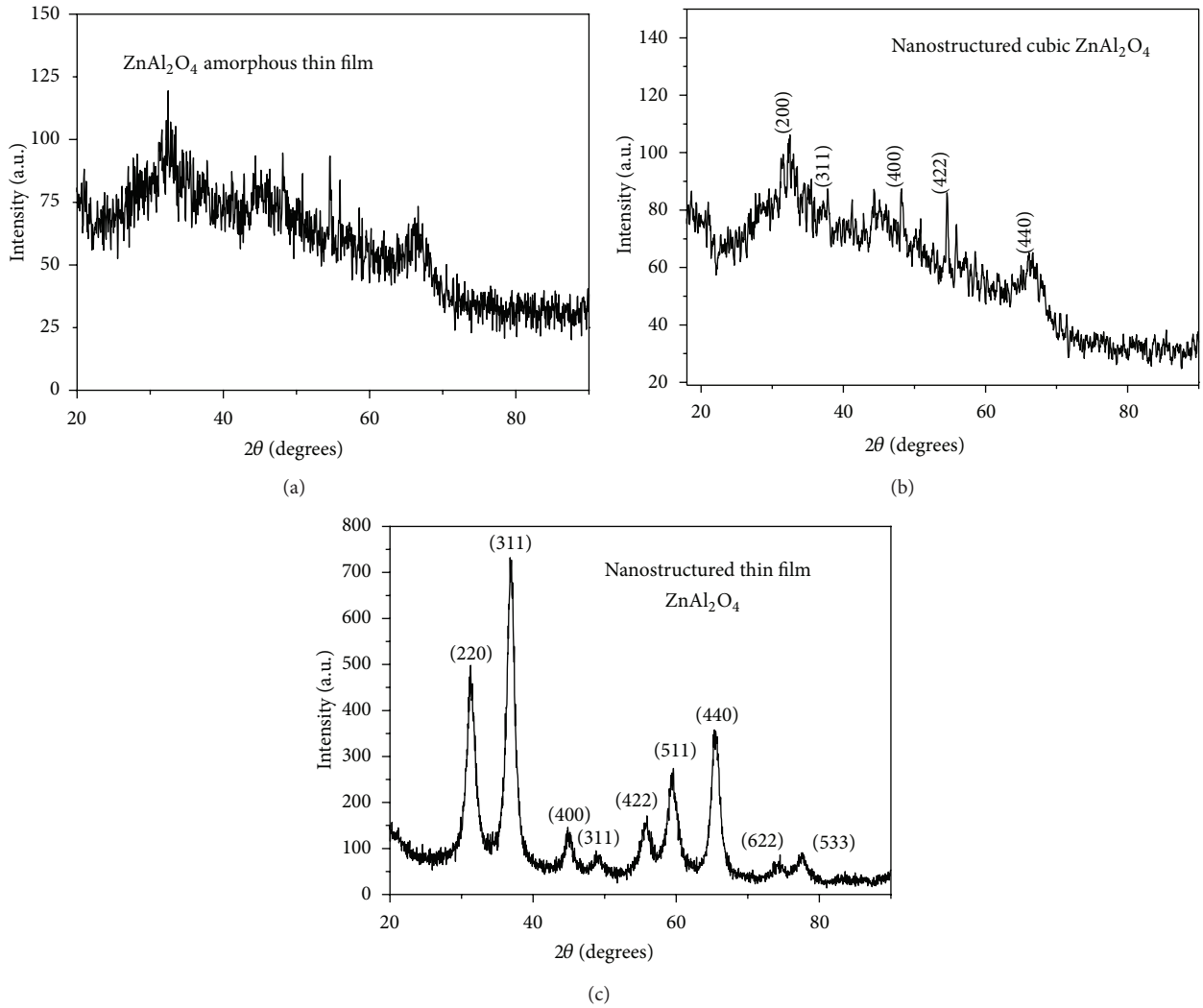

FIGURE 2: X-ray diffraction histograms of $ZnAl_2O_4$ thin films as a function of the T_s: (a) amorphous = 300°C, (b) nanostructured = 450°C, and (c) nanostructure = 550°C.

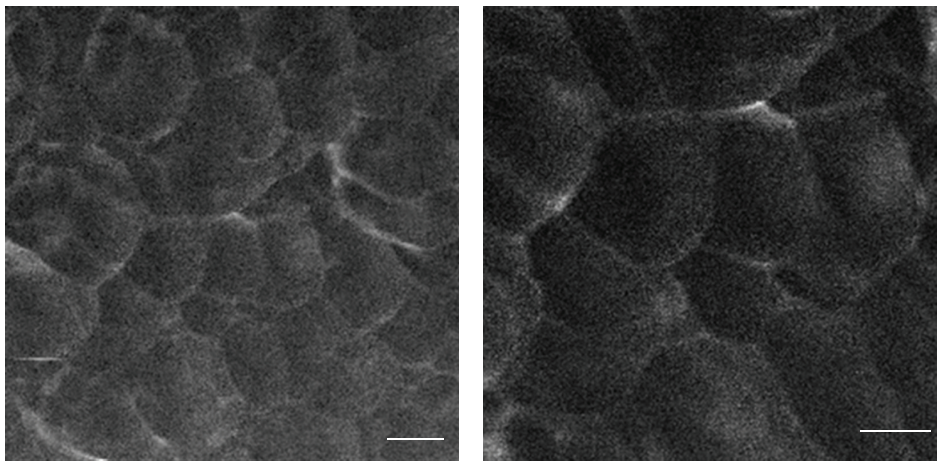

FIGURE 3: Surface morphology of the sintered pellets sample of $ZnAl_2O_4$. The surface is smooth, homogeneous (a), and without porous regions (b). Bar = 10 micron's.

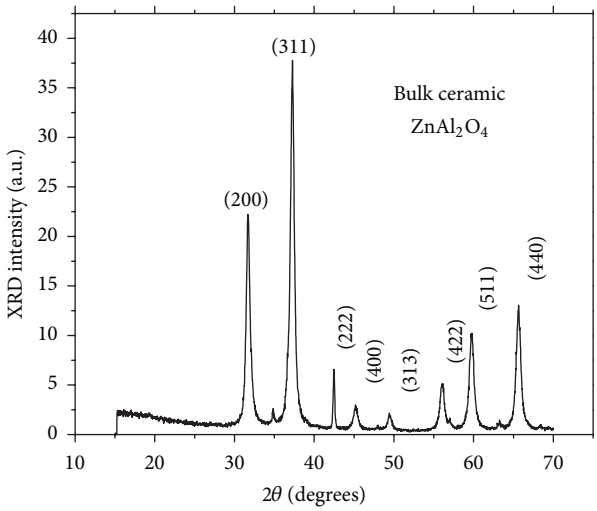

Figure 4: XRD of the bulk ceramic sample annealed at 600°C.

3. Results and Discussion

The surface morphology of $ZnAl_2O_4$ coatings deposited on glass substrates is presented in Figure 1. SEM micrographs show the samples deposited at 300°C Figure 1(a), 450°C Figure 1(b), and 550°C Figure 1(c). It is possible to observe rough but continuous coatings with good adherence to the substrate. This figure shows that the surface morphology of the layers depends on substrate temperature. Coatings deposited at 300°C and 450°C present some cracks. By increasing the substrate temperature to (500–550°C), the cracks disappear and a relatively more dense material is reached. These features could be explained because at higher substrate temperature, the deposited radicals are characterized by higher surface kinetic energy, which permits them better accommodation and consequently produces a better processed and compacted material.

At T_s = 550°C, the thin film shows a nanogranular morphology with a great quantity of porous regions, which mimics the surface morphology of the human bone.

The chemical composition of the films deposited at substrate temperature of 550°C was determined by EDS, with the atomic percentages of Zn = 13.6, Al = 27.8, O = 57.1, and Cl = 1.50, which means that we have $ZnAl_2O_4$ ceramic compound of stoichiometric composition doped with 1.50 % of chlorine.

XRD measurements carried out on the $ZnAl_2O_4$ coatings deposited by spray pyrolysis technique are presented in Figures 2(a), 2(b), and 2(c). These XRD patterns are shown for $ZnAl_2O_4$ at these three different substrate temperatures: 300°C, 450°C, and 550°C. The zinc aluminate coatings remain in the amorphous state when deposited at substrate temperatures up to 400°C (Figure 2(a)); as the substrate temperature is increased to 450°C, some peaks corresponding to hexagonal phase of ZnO (zincite, ICCD Card File no. 36-1451) are observed in Figure 2(b). In case of the sample deposited at 550°C Figure 2(c), only a cubic spinel crystalline phase of $ZnAl_2O_4$ (gahnite) was found (ICCD Card File no. 05-0669 [24]). The calculated lattice parameters ($a = b = c$ = 8.0859 Å) for the cubic spinel phase in the films deposited at 550°C are in agreement with the reported values ($a = b = c$ = 8.0848 Å) [24]. Furthermore, it promoted the crystal growth of this material with a preferential (311) orientation normal to the coatings surface. Considerable peaks broadening can be observed due to the nanometric dimension of the grains in the thin film. By using the Debye-Scherrer formula for the broadening fitting curve XRD program, the particle size was evaluated. The average particle diameter was around 20 ± 5 nm, considering that the grains are spheres.

The surface morphology of the polycrystalline $ZnAl_2O_4$ pellets sample obtained by chemical coprecipitation process is presented in Figure 3 and its XRD measurements pattern is shown in Figure 4. It is clear that this type of ceramic shows a smooth and homogeneous surface morphology without any observable porous region. Its average grain size is about 8.5 ± 2.0 μm.

The biomaterial surface interaction between scaffolds and tissue cells is a significant subject for biomaterials science. Information originating from this interaction is essential to aid the design and fabrication of new biocompatible materials [25]. Our results showed that when we culture osteoblastic cells on $ZnAl_2O_4$ nanostructured materials, the cell morphology had attached and undergone significant spreading, elongated demonstrating areas, where filopodia had intimately adapted with multiple cellular extensions on the surface of the ceramic (Figure 5(b)). In contrast, osteoblastic cells culture on $ZnAl_2O_4$ bulk materials showed neither or small elongation or extension (Figure 5(a)). These morphological results could be supported by the results of cell adhesion values after 4 and 24 h, presented as the cellular percentage of attached cells in relation to control tissue cultures plates. The cellular adhesion as the first step to assess the compatibility of the cell-material interaction surface was 60 to 80% greater on the $ZnAl_2O_4$ nanostructured material surface where it should be noted that the adherent values at all-time points were consistently higher when comparing with bulk ceramic surfaces (Figure 6). Statistical analyses indicated that there were statistically significant differences in the cell response, where osteoblastic cells attachment occurred preferred on the rough ceramic surface followed by the smooth surface ceramic. Moreover, it is important to remark that increased cellular attachment obtained on $ZnAl_2O_4$ bulk and 550°C thin film nanostructured materials is a good indicator that the surface is not toxic to the cells. We perform the cell viability test assessed by the MTT assay to confirm it. The results of the MTT assay are presented as the optical absorbance at 570 nm as shown in Figure 7. Both $ZnAl_2O_4$ nanostructure and bulk ceramics exhibited excellent biocompatibility. Among the two ceramics, it can be seen that cell viability is always higher on a nanostructured material than a bulk material, where we found high levels of MTT conversion and continue until day 7. This increment is directly proportional to the increase of metabolic active cells on the surface of $ZnAl_2O_4$ and inversely proportional to the toxicity effect of the surface topography of the material where significant differences in mean optical density are always presented as confirmed by Student's t-test. This increase in

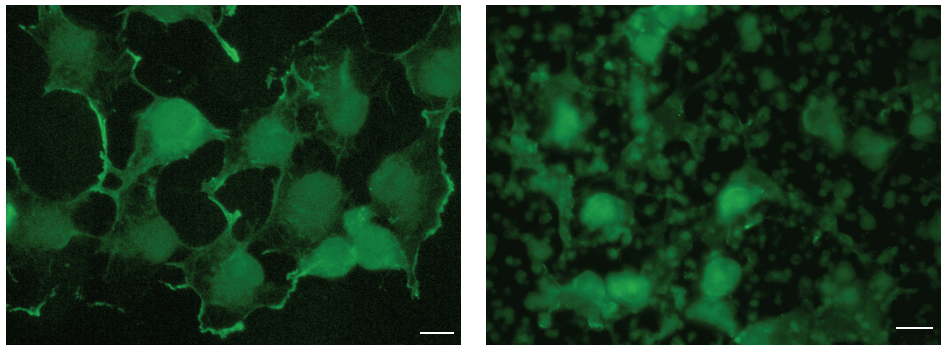

(a) (b)

FIGURE 5: Cytoskeletal organization morphology micrographs of the attachment of osteoblastic cells after 24 h on (a) bulk $ZnAl_2O_4$ ceramic and (b) $ZnAl_2O_4$ thin film nanostructured ceramic at $T_s = 550^{\circ}C$. Bar = 20 mm.

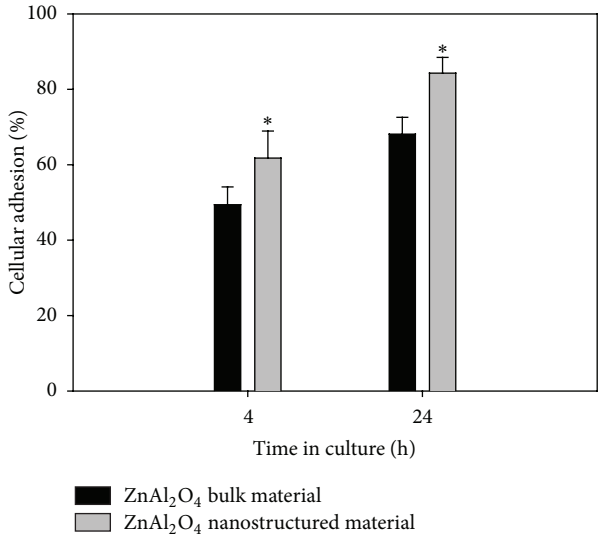

FIGURE 6: Quantitative cell adhesion of osteoblastic cells seeded on $ZnAl_2O_4$ (■) bulk material and (□) thin films nanostructure at $T_s = 550^{\circ}C$, after 4 and 24 h of culture, expressed as percent of cell attachment. Asterisk denotes significant differences ($P < 0.05$) between ceramic materials as determined by Student's t-test.

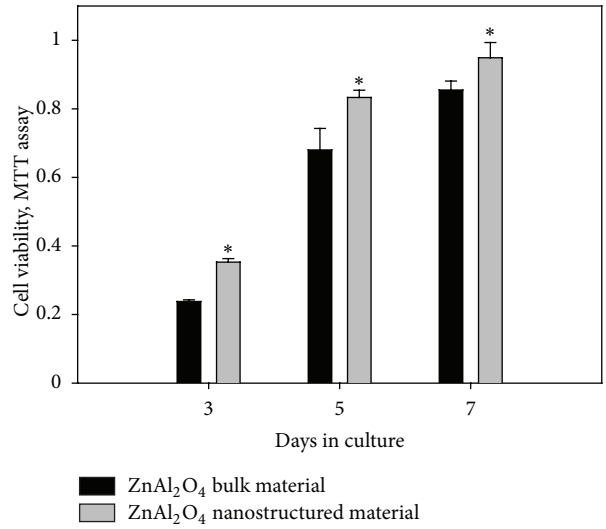

FIGURE 7: Cell viability determined by MTT assay after 3, 5, and 7 days of cell culture on $ZnAl_2O_4$ (■) bulk material and (□) thin films nanostructured at $T_s = 550^{\circ}C$. Error bars represent mean ± SE, $n = 3$ cultures under each conditions. Asterisk denotes significant differences ($P < 0.05$) between ceramic materials as determined by Student's t-test.

adhesion and viability by MTT activity of cells could be favored for the presence of $ZnAl_2O_4$ nanoparticle material. These results are in agreement with the idea that topography of extracellular microenvironment can influence cellular responses from attachment and migration to differentiation and production of new tissue [26–29]. Moreover, it has also been reported that surface energy is a more influential surface characteristic on cellular adhesion and proliferation [30, 31]. So the enhanced cellular adhesion and viability on $ZnAl_2O_4$ nanostructure ceramic could be due to the positive influence of the component of the surface energy. However, further studies are needed with these materials to fully understand the tissue cell-material interactions.

4. Conclusion

$ZnAl_2O_4$ nanostructure and bulk spinel ceramic have been evaluated for their *in vitro* biocompatibility to explore their potential to be used in dental implant and bone substitute applications. The *in vitro* attachment and morphological and viability responses of osteoblastic cells suggest that nanostructured ceramic appears to be the most conducive to cells compared to the bulk ceramic surface. The results of these studies could lead to a relatively new generation of bioceramics with surface characteristics specific to the needs of individual tissue types as bone or oral cavity.

Acknowledgments

The authors wish to thank Omar Novelo-Peralta, Raul Reyes, and Adriana Tejeda-Cruz from IIM-UNAM for their technical assistance during the course of this study. This study was supported by UNAM-DGAPA: (PAPIIT Grant no. 213912) and CONACYT (Grant no. 129780).

References

[1] R. J. Hill, J. R. Craig, and G. V. Gibbs, "Systematics of the spinel structure type," *Physics and Chemistry of Minerals*, vol. 4, no. 4, pp. 317–339, 1979.

[2] D. L. Anderson, "The earth as a planet: paradigms and paradoxes," *Science*, vol. 223, no. 4634, pp. 347–355, 1984.

[3] S. K. Sampath, D. G. Kanhere, and R. Pandey, "Electronic structure of spinel oxides: zinc aluminate and zinc gallate," *Journal of Physics Condensed Matter*, vol. 11, no. 18, pp. 3635–3644, 1999.

[4] S. Mathur, M. Veith, M. Haas et al., "Single-source sol-gel synthesis of nanocrystalline $ZnAl_2O_4$: structural and optical properties," *Journal of the American Ceramic Society*, vol. 84, no. 9, pp. 1921–1928, 2001.

[5] T. El-Nabarawy, A. A. Attia, and M. N. Alaya, "Effect of thermal treatment on the structural, textural and catalytic properties of the ZnO-Al_2O_3 system," *Materials Letters*, vol. 24, no. 5, pp. 319–325, 1995.

[6] H. Dinopoulos, R. Dimitriou, and P. V. Giannoudis, "Bone graft substitutes: what are the options?" *Surgeon*, vol. 10, no. 4, pp. 230–239, 2012.

[7] C. Zink, H. Hall, D. M. Brunette, and N. D. Spencer, "Orthogonal nanometer-micrometer roughness gradients probe morphological influences cell behavior," *Biomaterials*, vol. 33, no. 32, pp. 8055–8061, 2012.

[8] T. P. Kunzler, T. Drobek, M. Schuler, and N. D. Spencer, "Systematic study of osteoblast and fibroblast response to roughness by means of surface-morphology gradients," *Biomaterials*, vol. 28, no. 13, pp. 2175–2182, 2007.

[9] T. P. Kunzler, C. Huwiler, T. Drobek, J. Vörös, and N. D. Spencer, "Systematic study of osteoblast response to nanotopography by means of nanoparticle-density gradients," *Biomaterials*, vol. 28, no. 33, pp. 5000–5006, 2007.

[10] D. Khang, J. Choi, Y. M. Im et al., "Role of subnano-, nano- and submicron- surface features on osteoblast differentiation of bone marrow mesenchymal stem cells," *Biomaterials*, vol. 33, no. 26, pp. 5997–6007, 2012.

[11] P. Ducheyne and Q. Qiu, "Bioactive ceramics: the effect of surface reactivity on bone formation and bone cell function," *Biomaterials*, vol. 20, no. 23-24, pp. 2287–2303, 1999.

[12] M. Navarro, A. Michiardi, O. Castaño, and J. A. Planell, "Biomaterials in orthopaedics," *Journal of the Royal Society Interface*, vol. 5, no. 27, pp. 1137–1158, 2008.

[13] C. Wu, J. Chang, and W. Zhai, "A novel hardystonite bioceramic: preparation and characteristics," *Ceramics International*, vol. 31, no. 1, pp. 27–31, 2005.

[14] Y. Ramaswamy, C. Wu, H. Zhou, and H. Zreiqat, "Biological response of human bone cells to zinc-modified Ca-Si-based ceramics," *Acta Biomaterialia*, vol. 4, no. 5, pp. 1487–1497, 2008.

[15] H. Tapiero and K. D. Tew, "Trace elements in human physiology and pathology: zinc and metallothioneins," *Biomedicine and Pharmacotherapy*, vol. 57, no. 9, pp. 399–411, 2003.

[16] C. J. Boehlert and K. Knittel, "The microstructure, tensile properties, and creep behavior of Mg-Zn alloys containing 0–4.4 wt.% Zn," *Materials Science and Engineering A*, vol. 417, no. 1-2, pp. 315–321, 2006.

[17] M. Yamaguchi, H. Oishi, and Y. Suketa, "Stimulatory effect of zinc on bone formation in tissue culture," *Biochemical Pharmacology*, vol. 36, no. 22, pp. 4007–4012, 1987.

[18] Y. Tokudome and M. Otsuka, "Possibility of alveolar bone promotion enhancement by using lipophilic and/or hydrophilic zinc related copund in zinc deficient osteoporosis rats," *Biological & Pharmaceutical Bulletin*, vol. 35, no. 9, pp. 1496–1501, 2012.

[19] A. Ito, H. Kawamura, M. Otsuka et al., "Zinc-releasing calcium phosphate for stimulating bone formation," *Materials Science and Engineering C*, vol. 22, no. 1, pp. 21–25, 2002.

[20] Y. Tokudome, A. Ito, and M. Otsuka, "Effect of Zinc-containing b-tricalcium phosphate nanoparticles injection on jawbone mineral density and mechanical strength of osteoporosis model rats," *Biological & Pharmaceutical Bulletin*, vol. 34, no. 8, pp. 1215–1218, 2011.

[21] N. Saha, A. K. Dubey, and B. Basu, "Cellular proliferation, cellular viability, and biocompatibility of HA-ZnO composites," *Journal of Biomedical Materials Research B*, vol. 100, no. 1, pp. 256–264, 2012.

[22] J. C. Viguié and J. Spitz, "Chemical vapor deposition at low temperaturas," *Journal of the Electrochemical Society*, vol. 122, no. 4, pp. 585–588, 1975.

[23] H. Arzate, M. A. Alvarez-Pérez, M. E. Aguilar-Mendoza, and O. Alvarez-Fregoso, "Human cementum tumor cells have different features from human osteoblastic cells in vitro," *Journal of Periodontal Research*, vol. 33, no. 5, pp. 249–258, 1998.

[24] Power diffraction file card No. 05-0669, "International center for Diffraction Data," 1990.

[25] S. Chung and M. W. King, "Design concepts and strategies for tissue engineering scaffolds," *Biotechnology and Applied Biochemistry*, vol. 58, no. 6, pp. 423–438, 2011.

[26] O. Adamopoulos and T. Papadopoulos, "Nanostructured bioceramics for maxillofacial applications," *Journal of Materials Science*, vol. 18, no. 8, pp. 1587–1597, 2007.

[27] M. J. Dalby, D. McCloy, M. Robertson et al., "Osteoprogenitor response to semi-ordered and random nanotopographies," *Biomaterials*, vol. 27, no. 15, pp. 2980–2987, 2006.

[28] L. L. Hench and I. Thompson, "Twenty-first century challenges for biomaterials," *Journal of the Royal Society Interface*, vol. 7, no. 4, pp. S379–S391, 2010.

[29] D. F. Williams, "On the mechanisms of biocompatibility," *Biomaterials*, vol. 29, no. 20, pp. 2941–2953, 2008.

[30] B. Feng, J. Weng, B. C. Yang, S. X. Qu, and X. D. Zhang, "Characterization of surface oxide films on titanium and adhesion of osteoblast," *Biomaterials*, vol. 24, no. 25, pp. 4663–4670, 2003.

[31] P. Thevenot, W. Hu, and L. Tang, "Surface chemistry influences implant biocompatibility," *Current Topics in Medicinal Chemistry*, vol. 8, no. 4, pp. 270–280, 2008.